World Journal of Gastroenterology

Submit a Manuscript: http://www.wjgnet.com/esps/
Help Desk: http://www.wjgnet.com/esps/helpdesk.aspx
DOI: 10.3748/wjg.v23.i2.275

World J Gastroenterol 2017 January 14; 23(2): 275-285
ISSN 1007-9327 (print) ISSN 2219-2840 (online)

ORIGINAL ARTICLE

Retrospective Study

Pancreatic neuroendocrine neoplasms: Magnetic resonance imaging features according to grade and stage

Riccardo De Robertis, Sara Cingarlini, Paolo Tinazzi Martini, Silvia Ortolani, Giovanni Butturini, Luca Landoni, Paolo Regi, Roberto Girelli, Paola Capelli, Stefano Gobbo, Giampaolo Tortora, Aldo Scarpa, Paolo Pederzoli, Mirko D'Onofrio

Riccardo De Robertis, Department of Radiology, Casa di Cura Pederzoli, 37019 Peschiera del Garda, Italy

Riccardo De Robertis, Giampaolo Tortora, Course in Inflammation, Immunity and Cancer, University of Verona, 37134 Verona, Italy

Sara Cingarlini, Luca Landoni, Paola Capelli, Giampaolo Tortora, Aldo Scarpa, Mirko D'Onofrio, Verona Comprehensive Cancer Network, Department of Medical Oncology, G.B. Rossi Hospital, University of Verona, 37134 Verona, Italy

Paolo Tinazzi Martini, Department of Radiology, Casa di Cura Pederzoli, 37019 Peschiera del Garda, Italy

Silvia Ortolani, Department of Oncology, Casa di Cura Pederzoli, 37019 Peschiera del Garda, Italy

Giovanni Butturini, Paolo Regi, Roberto Girelli, Paolo Pederzoli, Department of Pancreatic Surgery, Casa di Cura Pederzoli, 37019 Peschiera del Garda, Italy

Stefano Gobbo, Department of Pathology, Casa di Cura Pederzoli, 37019 Peschiera del Garda, Italy

Author contributions: De Robertis R designed and performed the research and wrote the paper; D'Onofrio M designed the research and supervised the report; Cingarlini S, Tinazzi Martini P, Ortolani S, Butturini G, Landoni L, Regi P, Girelli R, Capelli P, Gobbo S, Tortora G, Scarpa A, Pederzoli P provided clinical advice and supervised the report.

Institutional review board statement: This study was approved by our institutional review board and the requirement for informed patient consent was waived due to the retrospective nature of the study.

Informed consent statement: Patients were not required to give informed consent to the study because the analysis used anonymous clinical data that were obtained after each patient agreed to MR examinations by written consent.

Conflict-of-interest statement: We have no financial relationships to disclose.

Data sharing statement: No additional data are available.

Manuscript source: Invited manuscript

Correspondence to: Riccardo De Robertis, MD, Department of Radiology, Casa di Cura Pederzoli, via Monte Baldo 24, 37019 Peschiera del Garda, Italy. riccardo.derobertis@hotmail.it
Telephone: +39-45-6449111
Fax: +39-45-6449223

Received: September 1, 2016
Peer-review started: September 2, 2016
First decision: October 20, 2016
Revised: November 7, 2016
Accepted: December 8, 2016
Article in press: December 8, 2016
Published online: January 14, 2017

Abstract

AIM

To describe magnetic resonance (MR) imaging features of pancreatic neuroendocrine neoplasms (PanNENs) according to their grade and tumor-nodes-metastases stage by comparing them to histopathology and to

determine the accuracy of MR imaging features in predicting their biological behavior.

METHODS

This study was approved by our institutional review board; requirement for informed patient consent was waived due to the retrospective nature of the study. Preoperative MR examinations of 55 PanNEN patients (29 men, 26 women; mean age of 57.6 years, range 21-83 years) performed between June 2013 and December 2015 were reviewed. Qualitative and quantitative features were compared between tumor grades and stages determined by histopathological analysis.

RESULTS

Ill defined margins were more common in G2-3 and stage Ⅲ-Ⅳ PanNENs than in G1 and low-stage tumors ($P < 0.001$); this feature had high specificity in the identification of G2-3 and stage Ⅲ-Ⅳ tumors (90.3% and 96%, 95%CI: 73.1-97.5 and 77.7-99.8). The mean apparent diffusion coefficient value was significantly lower in G2-3 and stage Ⅲ-Ⅳ lesions compared to well differentiated and low-stage tumors (1.09×10^{-3} mm^2/s *vs* 1.45×10^{-3} mm^2/s and 1.10×10^{-3} mm^2/s *vs* 1.53×10^{-3} mm^2/s, $P = 0.003$ and 0.001). Receiving operator characteristic analysis determined optimal cut-offs of 1.21 and 1.28×10^{-3} mm^2/s for the identification of G2-3 and stage Ⅲ-Ⅳ tumors, with sensitivity and specificity values of 70.8/80.7% and 64.5/64% (95%CI: 48.7-86.6/60-92.7 and 45.4-80.2/42.6-81.3).

CONCLUSION

MR features of PanNENs vary according to their grade of differentiation and their stage at diagnosis and could predict the biological behavior of these tumors.

Key words: Pancreatic neuroendocrine tumor; World Health Organization classification 2010; Diffusion-weighted imaging; European Neuroendocrine Tumor Society staging system; Magnetic resonance imaging

Core tip: This study aimed to describe magnetic resonance imaging features of pancreatic neuroendocrine neoplasms by comparing them to histopathology and to determine the accuracy in predicting tumor grade and biological behavior. Beside vascular infiltration and liver metastases, ill-defined margins had high specificity for the identification of G2-3 and stage Ⅲ-Ⅳ tumors (90.3% and 96%, respectively). Lesion size above 17.5 mm had a 91.7% sensitivity in the identification of G2-3 tumors; apparent diffusion coefficient values below 1.21 and 1.28×10^{-3} mm^2/s had high sensitivity (70.8% and 80.7%) for the identification of G2-3 and stage Ⅲ-Ⅳ tumors.

De Robertis R, Cingarlini S, Tinazzi Martini P, Ortolani S, Butturini G, Landoni L, Regi P, Girelli R, Capelli P, Gobbo S, Tortora G, Scarpa A, Pederzoli P, D'Onofrio M. Pancreatic neuroendocrine neoplasms: Magnetic resonance imaging features according to grade and stage. *World J Gastroenterol* 2017; 23(2): 275-285 Available from: URL: http://www.wjgnet.com/1007-9327/full/v23/i2/275.htm DOI: http://dx.doi.org/10.3748/wjg.v23.i2.275

INTRODUCTION

The biological behavior of pancreatic neuroendocrine neoplasms (PanNENs) is heterogeneous. The main adverse prognostic factors are the histopathological grade according to the World Health Organization (WHO) 2010 classification, which mainly relies on the proliferative activity[1], and the stage at diagnosis[2]. In fact, several studies demonstrated that high tumor grade and advanced tumor-nodes-metastases (TNM) stage are effective predictors of worse clinical outcome and shorter survival after surgical resection[3-5]. Moreover, tumor grade and stage influence the treatment strategy: surgical resection should always be considered if technically feasible, even in selected cases of metastatic disease; medical therapies are reserved to locally advanced or metastatic tumors in whom upfront surgery cannot be performed[5]. Pretreatment prediction of the biological behavior is therefore very important in determining an efficient treatment strategy for these tumors, especially when unresectable. Nevertheless, even invasive methods, as fine-needle aspiration (FNA), have a limited accuracy in determining the true proliferative activity of PanNENs[6]. Imaging methods could estimate the malignancy of PanNENs in a non-invasive way. In fact, previous studies have identified several imaging features that could predict the malignancy of these tumors: beside well-established criteria such as infiltration of peri-pancreatic vessels and liver metastases, other features associated with malignancy are large size, irregular margins, and hypoenhancement during the arterial phase[7-10]. Moreover, some authors reported that diffusion-weighted (DW) imaging, a technique that depicts and quantifies the random motion of water molecules within biological tissues on magnetic resonance (MR) imaging, might have the capability of roughly distinguish high grade PanNENs from G1 tumors[11-14]. Nevertheless, these results are based on small study populations and the diagnostic accuracy of imaging features in predicting the biological behavior of PanNENs is still undefined; moreover, in most previous studies tumor grade was established by FNA rather than histopathological analysis of surgical specimens. We therefore sought to investigate whether and how MR and DW imaging features could be useful in the non-invasive prediction of the biological behavior of PanNENs in a large cohort of patients who underwent surgery. As a consequence, the aims of this study are to describe MR and DW imaging features of PanNENs

according to the 2010 WHO grade classification and European Neuroendocrine Society (ENETS) TNM staging system by comparing them to histopathology and to determine the accuracy of MR imaging features in predicting the biological behavior of these tumors.

MATERIALS AND METHODS

Patient population

This study was approved by our institutional review board and the requirement for informed patient consent was waived due to the retrospective nature of the study.

A search of our histopathology and radiology records for the period June 2013-December 2015 revealed 66 patients with resected PanNEN, whose data were considered for inclusion. Inclusion criteria were: histopathological diagnosis of PanNEN after surgical resection and availability of good-quality preoperative MR examinations. Exclusion criteria were: lack of preoperative MR examinations (8 patients) and poor-quality MR examinations (3 patients).

Thirty subjects included in this study have been reported in a previous paper[14]; this prior article dealt with identification and characterization of PanNENs using MR and DW imaging, whereas in this manuscript we report on the correlation between MR and DW imaging findings, tumor grade and biological behavior expressed as the stage at diagnosis.

The final study population comprised 55 patients with a mean age of 57.6 years (range, 21-83 years): 29 men (mean age, 58.2 years; range, 35-83 years) and 26 women (mean age, 57 years; range, 21-77 years).

At histopathological examination of surgical specimens, 31 tumors (56.4%) were classified as G1, 20 (36.4%) as G2, and 4 (7.2%) as G3, according to the 2010 WHO classification[1].

Four patients underwent tumor enucleation or middle pancreatectomy without lymphadenectomy, therefore the TNM classification could not be applied; accordingly, the remaining 51 lesions were staged as follows, according to the ENETS TNM classification[15]: stage Ⅰ, 15 lesions (29.4%); stage ⅡA or B, 10 lesions (19.6%); stage ⅢA or B, 19 lesions (37.2%); stage Ⅳ, 7 lesions (13.7%).

MR imaging

All patients signed an informed consent before MR examination. MR imaging was performed in a single institution using a 1.5 T unit (Magnetom Avanto or Aera; Siemens, Erlangen, Germany) using phased-array body coils. The patients were asked to fast for 4-6 h before MR. One hundred mL of pineapple juice were administered 10-20 min before MR to prevent signal overlapping from fluid-containing organs on T2-weighted images. The MR imaging protocol is reported in Table 1. For DWI, *b*-values of 50, 400 and 800 s/mm^2 were used. DW images were acquired using a free-breathing echo-planar sequence; apparent diffusion coefficient (ADC) maps were obtained with a monoexponential decay model. Contrast-enhanced MR imaging involved a quadriphasic study; 0.1 mmol of a gadolinium chelate (gadobenate dimeglumine, MultiHance; Bracco, Milan, Italy) per kilogram of body weight were administered at 2.0-2.5 mL/s by using a power injector (Medrad, Pittsburgh, Pa., United States). Images were obtained before contrast material administration and during the late arterial/pancreatic, portal/venous and delayed phases (35-45, 75-80 and > 180 s after the start of contrast material administration).

Image analysis

Qualitative and quantitative MR features of each tumor were retrospectively analyzed on a workstation by two radiologists (RDR and PTM, with 6 and 26 years of experience in abdominal radiology); discrepancies were solved by consensus. Aside from knowing that the patients had PanNENs, both readers were blinded to all other histopathological features. The qualitative image analysis included: (1) location of the lesion; (2) margins; (3) presence of intratumoral cystic/necrotic areas; (4) main pancreatic duct (MPD) and/or common bile duct (CBD) dilation upstream to the lesion; (5) atrophy of the upstream parenchyma; (6) involvement of peripancreatic vessels; (7) liver metastases; (8) signal intensity of the lesion related to the adjacent parenchyma (hypo-, iso- or hyperintense); and (9) type of enhancement (homogeneous or heterogeneous). Quantitative image analysis included: (1) maximum diameter of the lesion; (2) caliber of the MPD/CBD upstream to the lesion; and (3) mean ADC values of the tumor. Pancreatic tail tumors were excluded from the evaluation of MPD features and pancreatic atrophy; pancreatic body/tail lesions were excluded from the evaluation of CBD dilation and caliber. ADC quantification was performed drawing multiple free-hand regions of interests on several contiguous axial slices to include nearly the whole tumor volume; the results were averaged to obtain the mean ADC value. Care was taken during ROI placement to avoid inhomogeneities; each ROI was positioned slightly inside the outer edge of each lesion, thereby preventing partial volume artifacts. The positioning of the ROI was performed in correlation with the other sequences.

Statistical analysis

For the purpose of statistical analysis, G2 and G3 tumors, as well as stage Ⅲ and stage Ⅳ PanNENs were grouped and considered together.

Categorical variables derived from the qualitative analysis were compared between groups using the χ^2 or Fisher's exact tests; the results are presented as numbers of cases and relative frequencies. Continuous

Table 1 Magnetic resonance protocol and pulse sequences: Technical parameters

Pulse sequence	Imaging plane	TR (ms)	TE (ms)	Thickness (mm)
T2w HASTE	Axial	∞	90.00	6
	Coronal	∞	90.00	6
	Para-coronal	∞	90.00	4
	Sagittal	∞	90.00	4
FsT2w RARE	Axial	2900.00	82-87	6
DWI-EPI	Axial	6000-6500	59.00	6
Chemical-shift	Axial	90-130	2.37/4.87	6
FsT1w VIBE	Axial	4.28	2.39	2-3
	Coronal	3.52	1.32	2-3
	Sagittal	3.52	1.32	2-3
2D MRCP HASTE	Multiple	∞	746.00	65-75

TR: Repetition time; TE: Time of echo; HASTE: Half-Fourier single-shot turbo spin echo; DWI-EPI: Diffusion-weighted echo-planar imaging; RARE: Rapid acquisition with relaxation enhancement; VIBE: Volume-interpolated breath-hold examination; MRCP: Magnetic resonance cholangiopancreatography.

variables derived from the quantitative analysis were compared between groups using Student's *t* test or univariate ANOVA; the results are reported as mean ± SD. Student's *t* tests and bivariate correlation tests were conducted to assess whether qualitative and quantitative variables were correlated with tumor size. For each significant qualitative feature, the diagnostic performance in the identification of G2-3 and stage Ⅲ-Ⅳ lesions was tested by calculating sensitivity (Se, %), specificity (Sp, %), positive and negative predictive values (PPV/NPV, %). A receiving operator characteristic (ROC) analysis evaluated the diagnostic performance of significant quantitative features, and optimal cut-off values, along with Se, Sp, and PPV/NPV, were thus ascertained. Diagnosis obtained by pathological examination was the external gold standard. The sensitivity and specificity of combinations of the statistically significant MR criteria were also calculated. Statistical analysis was performed with SPSS software version 21.2 (IBM, Chicago, Ill., United States). All *P* values were considered statistically significant if $\leqslant$ 0.05.

RESULTS

Qualitative and quantitative features

Details on the qualitative features are reported in Tables 2 and 3. Most lesions were located in the body or in the head of the pancreas, without significant differences in terms of location between tumor grades and stages (*P* = 0.094 and 0.059, respectively). Most tumors presented well defined margins; among tumors presenting ill-defined margins, most were found to be G2-3 (13/16; Figure 1) or stage Ⅲ-Ⅳ (15/16) at histopathological analysis, with significantly higher frequency when compared to G1 and stage Ⅰ-Ⅱ tumors (81.2% *vs* 18.8% and 93.8% *vs* 6.2%, *P* < 0.001). A significantly higher proportion of G2-3 tumors presented infiltration of peri-pancreatic vessels and liver metastases compared to G1 tumors (25% *vs* 3.2% and 29.2% *vs* 0%, *P* = 0.022 and 0.002, respectively; Figure 2). Atrophy of upstream pancreatic parenchyma and dilation of the MPD/CBD were more common among G2-3 tumors and stage Ⅲ-Ⅳ lesions as compared to G1 and stage Ⅰ-Ⅱ tumors, although without significant differences between groups (*P* = 0.446/0.151, 0.215/0.151, and 0.264/0.275).

Most lesions were hypointense on T1- and T1fs-weighted images, hyper- or isointense on T2w images and hyperintense on fsT2w images. On post-contrast images, most tumors were hyperenhancing on late arterial/pancreatic and portal phase images; most tumors of this series were iso- or hyperintense on delayed phase images. No significant differences between tumor grades and stages were found regarding the signal intensity on both unenhanced and post-contrast images. Intratumoral fluid areas were more frequently found within G2-3 PanNENs, albeit without significant differences between tumor grades and stages (*P* = 0.279 and 0.464). Heterogeneous enhancement was significantly more common among G2-3 tumors as compared to G1 lesions (*P* = 0.006); nevertheless, lesions with heterogeneous enhancement were significantly larger than those presenting homogeneous enhancement, independently from tumor grade (39.3 ± 23.5 mm *vs* 19.8 ± 12.8 mm, *P* < 0.001).

Details on the results of the qualitative image analysis and the comparison between grades and ENETS TNM stages are reported in Table 4. The lesions had a mean diameter of 28.7 ± 20.8 mm; G2-3 tumors were significantly larger than G1 PanNENs (*P* = 0.017), while no significant differences were found between tumor stages in terms of size (*P* = 0.080). The mean caliber of the MPD/CBD was 6 ± 2 and 13.4 ± 3.9 mm, respectively; no significant differences between tumor grades were found regarding the extent of MPD/CBD dilation (*P* = 0.256 and 0.151, respectively), while the MPD/CBD diameter was significantly larger in stage I-II PanNENs as compared to stage Ⅲ-Ⅳ tumors (*P* = 0.038 and 0.034, respectively). G2-3 and stage Ⅲ-Ⅳ PanNENs presented significantly lower mean ADC values compared to G1 and stage Ⅰ-Ⅱ tumors (1.09 ± 0.28 × 10^{-3} mm^2/s *vs* 1.45 ± 0.53 × 10^{-3} mm^2/s and 1.10 ± 0.25 × 10^{-3} mm^2/s *vs* 1.53 ± 0.55 × 10^{-3} mm^2/s; *P* = 0.003 and 0.001, respectively; Figure 3). ADC values were not correlated to tumor size (*P* = 0.236).

Performances of MR features in predicting the biological behavior

The diagnostic performance of MR imaging parameters in identifying G2-3 and stage Ⅲ-Ⅳ PanNENs is presented in Table 5. Among qualitative features, vascular invasion and liver metastases had the highest specificity in identifying G2-3 tumors (96.7%, 95%CI: 81.5-99.8). Ill-defined margins had high specificity for the identification of G2-3 and stage Ⅲ-Ⅳ PanNENs

Table 2 Comparison of qualitative features between grades and stages

Feature	Grade				ENETS TNM stage[1]			
	Total	G1[2]	G2-3[2]	*P* value	Total	I / II[2]	III/IV[2]	*P* value
Location				0.094				0.059
Head	24	11 (45.8)	13 (54.2)		23	7 (30.4)	16 (69.6)	
Body	25	18 (72)	7 (28)		22	14 (63.6)	8 (36.4)	
Tail	6	2 (33.3)	4 (66.7)		6	4 (66.7)	2 (33.3)	
Margins				< 0.001				< 0.001
Well defined	39	28 (71.8)	11 (28.2)		35	24 (68.6)	11 (31.4)	
Ill defined	16	3 (18.8)	13 (81.2)		16	1 (6.2)	15 (93.8)	
Vasc. infiltration				0.022	-	-	-	-
Present	7	1 (14.3)	6 (85.7)					
Absent	48	30 (62.5)	18 (37.5)					
Liver metastases				0.002	-	-	-	-
Present	7	0 (0)	7 (100)					
Absent	48	31 (64.6)	17 (35.4)					
Atrophy[3]				0.446				0.151
Present	13	7 (53.8)	6 (46.2)		13	4 (30.8)	9 (69.2)	
Absent	36	22 (61.1)	14 (38.9)		32	17 (53.1)	15 (46.9)	
MPD dilation[4]				0.215				0.151
Present	13	6 (46.2)	7 (53.8)		13	4 (30.8)	9 (69.2)	
Absent	36	23 (63.9)	13 (36.1)		32	17 (53.1)	15 (46.9)	
CBD dilation[4]				0.264				0.275
Present	7	2 (28.6)	5 (71.4)		7	1 (14.3)	6 (85.7)	
Absent	17	9 (52.9)	8 (47.1)		16	6 (37.5)	10 (62.5)	

[1]Four lesions were excluded from this analysis (minimally invasive surgery without lymphadenectomy); [2]Number of cases/cases in row; [3]Pancreatic head/body lesions; [4]Pancreatic head lesions. Data are presented as numbers of cases. ENETS: European Neuroendocrine Society; TNM: Tumor-nodes-metastases.

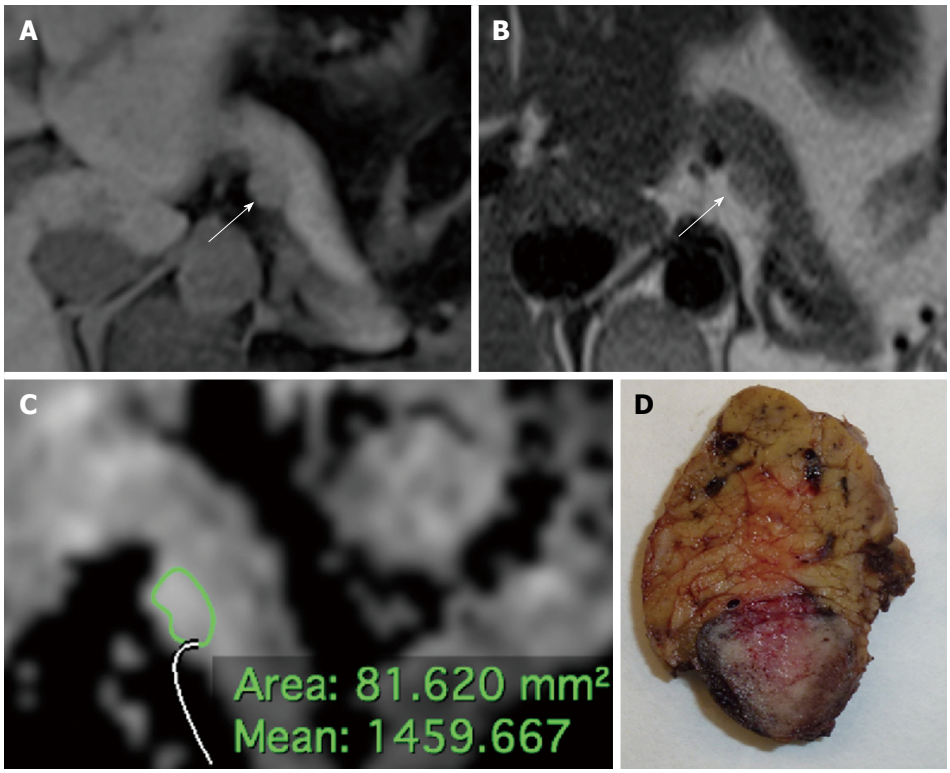

Figure 1 Small hyperfunctioning pancreatic neuroendocrine neoplasm (insulinoma) classified as G1, stage 1 tumor at histology (Ki67 < 1%, T1, N0, M0) in a 44 years-old woman. A: Axial volumetric interpolated breath-hold examination (VIBE) gradient echo image (repetition time msec/echo time msec, 4.3/1.4) with fat suppression shows a homogeneously hypointense lesion with well defined margins (arrow) in the pancreatic body; B: On axial T2-weighted half-Fourier single-shot turbo spin echo (HASTE) image (TR/TE, ∞/90), the tumor appears slightly hyperintense (arrow) compared to adjacent pancreatic parenchyma; C: At ADC quantification the tumor had a relatively high mean ADC value; D: The macroscopic pathological specimen (distal pancreatectomy, sagittal cut) shows a small, well-delimitated lesion bulging the contour of the pancreatic body.

Table 3 Comparison of signal intensity between grades and European Neuroendocrine Society tumor-nodes-metastases stages

Feature	Grade				ENETS TNM stage[1]			
	Total	G1[2]	G2-3[2]	*P* value	Total	I / II[2]	III/IV[2]	*P* value
T1w				0.395				0.659
Hypointense	45	27 (60)	18 (40)		42	22 (52.4)	20 (47.6)	
Isointense	4	1 (25)	3 (75)		4	1 (25)	3 (75)	
Hyperintense	6	3 (50)	3 (50)		5	2 (40)	3 (60)	
fsT1w				0.836				0.900
Hypointense	39	23 (59)	16 (41)		37	19 (51.4)	18 (48.6)	
Isointense	9	5 (55.6)	4 (44.4)		8	3 (37.5)	5 (62.5)	
Hyperintense	7	3 (42.9)	4 (57.1)		6	3 (50)	3 (50)	
T2w				0.937				0.274
Hypointense	16	9 (56.3)	7 (43.2)		16	8 (50)	8 (50)	
Isointense	12	6 (50)	6 (50)		11	3 (27.3)	8 (72.7)	
Hyperintense	27	16 (59.3)	11 (40.7)		24	14 (58.3)	10 (41.7)	
fsT2w				1.000				0.318
Hypointense	13	7 (53.8)	6 (46.2)		13	5 (38.5)	8 (61.5)	
Isointense	11	6 (54.5)	5 (45.5)		9	3 (33.3)	6 (66.7)	
Hyperintense	31	18 (58.1)	13 (41.9)		29	17 (58.6)	12 (41.4)	
Fluid areas				0.279				0.464
Present	15	7 (46.7)	8 (53.3)		15	8 (53.3)	7 (46.7)	
Absent	40	24 (60)	16 (40)		38	17 (47.2)	19 (52.8)	
Arterial				0.089				0.055
Hypointense	13	4 (30.8)	9 (69.2)		12	3 (25)	9 (75)	
Isointense	11	8 (72.7)	3 (27.3)		9	3 (33.3)	6 (66.7)	
Hyperintense	31	19 (61.3)	12 (38.7)		30	19 (63.3)	11 (36.7)	
Portal				1.000				0.933
Hypointense	14	8 (57.1)	6 (42.9)		14	6 (42.9)	8 (57.1)	
Isointense	13	7 (53.8)	6 (46.2)		12	6 (50)	6 (50)	
Hyperintense	28	16 (57.1)	12 (42.9)		25	13 (52)	12 (48)	
Delayed				0.441				0.340
Hypointense	12	6 (50)	6 (50)		11	4 (36.4)	7 (63.6)	
Isointense	19	9 (47.4)	10 (52.6)		17	7 (41.2)	10 (58.8)	
Hyperintense	24	16 (66.7)	8 (33.3)		23	14 (60.9)	9 (39.1)	
Enhancement				0.006				0.163
Heterogeneous	25	9 (36)	16 (64)		25	10 (40)	15 (60)	
Homogeneous	30	22 (73.3)	8 (26.7)		26	15 (57.7)	11 (42.3)	

[1]Four lesions were excluded from this analysis (minimally invasive surgery without lymphadenectomy); [2]Number of cases/cases in row. ENETS: European Neuroendocrine Society; TNM: Tumor-nodes-metastases.

Table 4 Qualitative image analysis and comparison between grades and stages

	Grades				ENETS TNM stages[1]			
	Total	G1	G2-3	*P* value	Total	I / II	III/IV	*P* value
Size (mm)	28.7 ± 20.8	22.7 ± 17.7	36.4 ± 22.1	0.017	29.9 ± 21.1	24.6 ± 19	34.9 ± 22.1	0.080
MPD caliber[2] (mm)	6 ± 2	6.8 ± 2.7	5.4 ± 1	0.256	6 ± 2	7.7 ± 2.9	5.3 ± 0.9	0.038
CBD caliber[3] (mm)	13.4 ± 3.9	18.3 ± 3	11.5 ± 2	0.151	13.4 ± 3.9	20.5	12.3 ± 2.6	0.034
ADC_L ($\times 10^{-3}$ mm^2/s)	1.29 ± 0.47	1.45 ± 0.53	1.09 ± 0.28	0.003	1.31 ± 0.48	1.53 ± 0.55	1.10 ± 0.25	0.001

Data are expressed as means ± SD. [1]Four lesions have been excluded from this analysis (minimally invasive surgery without lymphadenectomy); [2]Pancreatic head/body lesions showing upstream MPD dilation; [3]Pancreatic head lesions showing upstream CBD dilation. ENETS: European Neuroendocrine Society; TNM: Tumor-nodes-metastases.

(90.3% and 96%, 95%CI: 73.1-97.5 and 77.7-99.8, respectively; Figure 2). The ROC analysis of lesions' size provided an area under the curve (AUC) for the identification of G2-3 tumors of 0.757; the best cut-off value was found to be 17.5 mm, which provided a sensitivity of 91.7% (95%CI: 71.5-98.5) and a specificity of 61.3 (95%CI: 42.3-77.6).

By excluding 8 hyperfunctioning tumors and increasing the size threshold to 20 mm, a previously identified cutoff for the choice between surgical resection and follow-up[5], the AUC was found to be 0.736, sensitivity dropped to 79.2% (95%CI: 57.3-92.1), while specificity remained substantially unchanged (60.9%, 95%CI: 38.8-79.5). The ROC analysis of ADC values provided an AUC value of 0.740 for the identification of G2-3 tumors; the best cut-off value for the identification of G2-3 tumors was found to be 1.21 × 10^{-3} mm^2/s, that yielded a sensitivity of 70.8% (95%CI: 48.7-86.6) and a specificity of 64.5% (95%CI: 45.4-80.2). The ROC analysis of ADC values

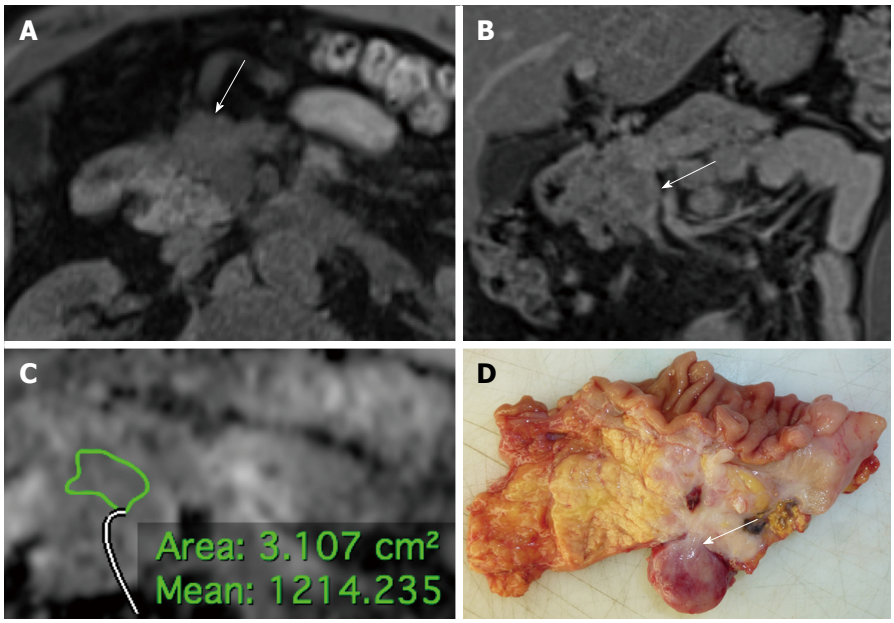

Figure 2 Non-hyperfunctioning pancreatic neuroendocrine neoplasm of the pancreatic head classified as G2, stage 3b tumor at histology (Ki67 15%, T4, N1, M0) in a 55 years-old man. A: Axial volumetric interpolated breath-hold examination (VIBE) gradient echo image (repetition time msec/echo time msec, 4.3/1.4) with fat suppression shows a hypointense tumor with ill-defined margins (arrow); B: On coronal fat-saturated T1-weighted volumetric interpolated breath-hold examination (VIBE) gradient echo image (TR/TE 3.5/1.3 ms) acquired during the delayed phase of the dynamic study the tumor shows heterogeneous contrast enhancement, with infiltration of the superior mesenteric vein (arrow); C: The tumor presents intermediate mean ADC value; D: The surgical specimen (pancreaticoduodenectomy with *en bloc* resection of the superior mesenteric vein, transverse cut) shows a large lesion of the pancreatic head with irregular margins infiltrating the superior mesenteric vein (arrow).

Table 5 Diagnostic performances in the identification of G2-3 and stage Ⅲ-Ⅳ pancreatic neuroendocrine neoplasms

	Feature	Diagnostic performance			
		Se	Sp	PPV	NPV
Grade 2-3	Ill defined margins	54.2 (33.2-73.8)	90.3 (73.1-97.5)	81.2 (53.7-95)	71.7 (54.9-84.4)
	Vascular infiltration	29.2 (13.4-51.2)	96.7 (81.5-99.8)	87.5 (46.7-99.3)	63.8 (48.4-76.9)
	Liver metastases	25 (10.6-47)	96.7 (81.5-99.8)	85.7 (42-99.2)	62.5 (47.3-75.7)
	Heterogeneous enhancement	66.7 (44.7-83.6)	71 (51.7-85.1)	64 (42.6-81.3)	73.3 (53.8-87)
	Size > 17.5 mm	91.7 (71.5-98.5)	61.3 (42.3-77.6)	64.7 (46.5-79.7)	90.5 (68.2-98.3)
	Size > 20 mm	79.2 (57.3-92.1)	60.9 (38.8-79.5)	67.8 (47.6-83.4)	73.6 (48.6-52.4)
	ADC < 1.21 × 10^{-3} mm^2/s	70.8 (48.7-86.6)	64.5 (45.4-80.2)	60.7 (40.7-77.9)	74.1 (53.4-88.1)
Stage Ⅲ-Ⅳ	Ill defined margins	57.7 (37.2-76)	96 (77.7-99.8)	93.7 (67.7-99.7)	68.6 (50.6-82.6)
	ADC < 1.28 × 10^{-3} mm^2/s	80.7 (60-92.7)	64 (42.6-81.3)	70 (50.4-84.6)	76.2 (52.4-90.9)

Diagnostic performances are expressed as percentages (95%CI). AUC: Area under the curve; Se: Sensitivity; Sp: Specificity; PPV: Positive predictive value; NPV: Negative predictive value.

for the identification of stage Ⅲ-Ⅳ tumors provided an AUC of 0.773; the best cut-off value for the identification of stage Ⅲ-Ⅳ tumors was found to be 1.28 × 10^{-3} mm^2/s (sensitivity 80.7%, 95%CI: 60-92.7; specificity 64%, 95%CI: 42.6-81.3).

Details regarding the diagnostic accuracy of different combinations of MR features in diagnosing G2-3 tumors are reported in Table 6. The highest sensitivity and specificity were reached using at least two of these five criteria in combination (79.2%, 95%CI: 57.3-92.1; and 80.6%, 95%CI: 61.9-91.9); in particular, the highest specificity values (100%) in diagnosing G2-3 tumors were reached using a combination of ill-defined margins and vascular involvement and/or liver metastases and ill-defined margins.

DISCUSSION

PanNENs have a wide variety of biological behavior. Although all PanNENs have a malignant potential, the biologic aggressiveness and metastasizing risk are variable. The 2010 WHO classification categorize PanNENs into three classes based on their mitotic activity, expressed as mitotic rate or Ki-67 index: G1, < 2 mitoses/2 mm^2 (10 high power fields, 40× magnification) and/or a Ki-67 index ⩽ 2%; G2, 2-20 mitoses/2 mm^2 and/or a Ki-67 index between 3% and 20%, and G3, ⩾ 21 mitoses/2 mm^2 and a Ki-67 index > 20%[1,15]. Previous studies demonstrated that Ki-67 value is an independent predictor of survival for PanNENs[16]. Strosberg *et al*[17] reported 5-year

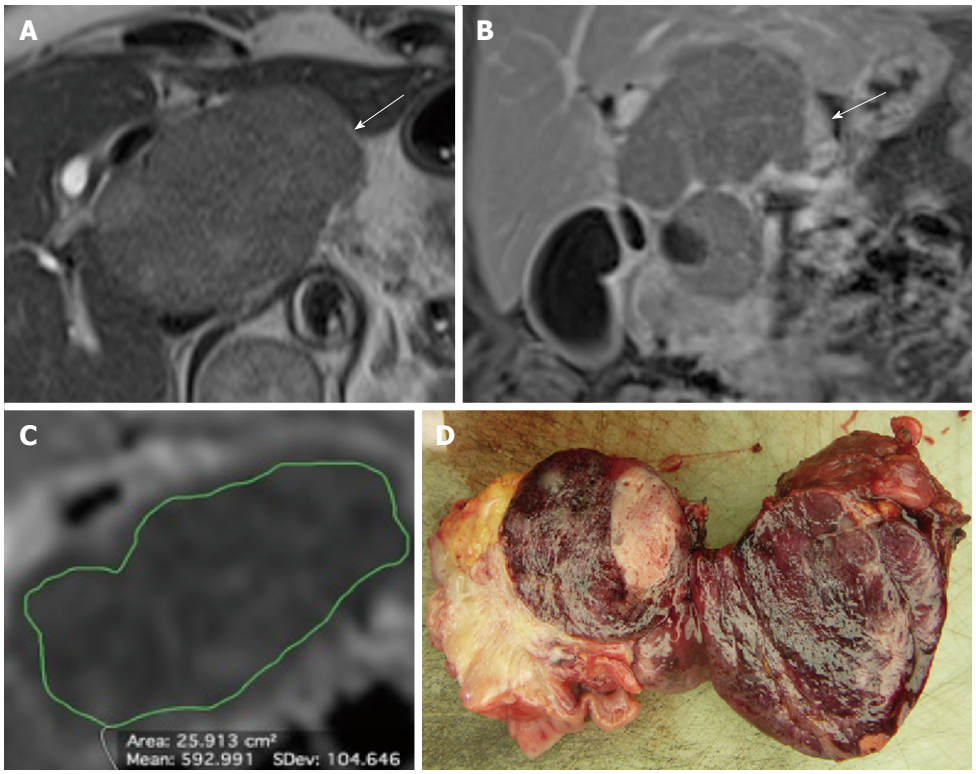

Figure 3 Non-hyperfunctioning pancreatic neuroendocrine neoplasm of the pancreatic head classified as G3, stage 3b tumor at histology (Ki67 60%, T4, N1, M0) in a 76 years-old woman. A: Axial T2-weighted half-Fourier single-shot turbo spin echo (HASTE) image (TR/TE, ∞/90) shows a large, slightly hyperintense tumor in the pancreatic head (arrow); B: On coronal fat-saturated T1-weighted volumetric interpolated breath-hold examination (VIBE) gradient echo image (TR/TE 3.5/1.3 ms) acquired during the delayed phase of the dynamic study the tumor shows heterogeneous contrast enhancement (arrow); C: At quantitative analysis of ADC map the tumor shows low mean ADC value; D: The surgical specimen (pancreaticoduodenectomy, sagittal cut) shows a large lesion of the pancreatic head with heterogeneous aspect.

Table 6 Combination of magnetic resonance findings for differentiating G1 from G2-3 pancreatic neuroendocrine neoplasms

Number of features	Diagnostic performance			
	Se	Sp	PPV	NPV
≥ 1	100 (82.8-100)	35.5 (19.8-54.6)	54.5 (38.9-69.3)	100 (67.8-100)
≥ 2	79.2 (57.3-92.1)	80.1 (61.9-91.9)	76 (54.5-89.8)	83.3 (64.5-93.7)
≥ 3	58.3 (36.9-77.2)	93.5 (77.1-98.9)	87.5 (60.4-97.8)	74.3 (57.6-86.4)
≥ 4	20.8 (7.9-42.7)	96.7 (81.5-99.8)	83.3 (36.5-99.1)	61.2 (46.2-74.4)
≥ 5	8.3 (1.4-28.5)	96.4 (86.4-99.4)	100 (19.8-100)	58.5 (44.2-71.6)

MR findings are ill-defined margins, vascular invasion, liver metastases, size > 17.5 mm, ADC < 1.21 < 10^{-3} mm^2/s. Diagnostic performances are expressed as percentages (95%CI). Se: Sensitivity; Sp: Specificity; PPV: Positive predictive value; NPV: Negative predictive value.

survival rates for patients with low-, intermediate-, and high-grade metastatic tumors of 87%, 38%, and 0%, respectively. Along with tumor grade, the stage according to the ENETS TNM classification represent an adverse prognostic factor of PanNENs: as reported by Yang *et al*[18], the 5-year survival rates for the stages Ⅰ, Ⅱ, Ⅲ, and Ⅳ were 75.5%, 72.7%, 29.0%, and not-assessable, respectively. Rindi *et al*[2] reported that the ENETS TNM staging system perfectly allocated patients into four statistically significantly different and equally populated risk groups, with stage Ⅱ hazard ratio (HR) of death equal to 16.23, stage Ⅲ HR of death of 51.81, and stage Ⅳ HR of death of 160, considering stage Ⅰ as the reference. It is still controversial which, between tumor grade and stage, has a greater influence on survival. At this regard, a study conducted by Martin-Perez *et al*[3] reported that patients with surgically resected loco regional disease and high Ki-67 index (> 20%) had worse prognosis (17% 5-year survival rate) than those with advanced disease but low proliferative index (63% 5-year survival rate). These data suggest that Ki-67 index have a greater impact on survival than the extent of disease. The treatment of choice for PanNENs is surgical resection, which should always be considered if technically feasible, even in selected cases of metastatic disease[5]; medical therapies, including chemotherapy, antiangiogenic drugs and peptide receptor radionuclide therapy, are reserved to locally advanced or metastatic tumors in whom upfront surgical resection cannot be

performed. Small (< 20 mm) non-hyperfunctioning PanNENs have a low malignant potential, therefore a follow-up strategy can be adopted in such cases[5]. The treatment strategy of PanNENs, however, differs according to their malignancy. Therefore, the more precise will be the pretreatment prediction of the biological behavior of PanNENs, the more effective will be their treatment. In this setting, besides the well-established criteria of malignancy such as the infiltration of peri-pancreatic vessels and liver metastases, a parameter associated with malignancy is tumor size[7,8]. In our series, G2-3 tumors were significantly larger than G1 PanNENs (36.7 mm *vs* 22.6 mm, $P = 0.022$); the optimal size cut-off for the identification of G2-3 tumors was found to be 17.5 mm, a value that yielded a sensitivity of 91.7%. As previously mentioned, a non-operative management has been advocated for non-hyperfunctioning tumors below 20 mm when discovered incidentally[5]; in the present study, after the exclusion of 8 hyperfunctioning PanNENs from our sample population, a cut-off value of 20 mm provided a sensitivity of 79.2% for the identification of G2-3 tumors. Ill-defined margins are significantly associated with aggressive lesions[9]; in our series, ill-defined margins were significantly more common among high-grade and high-stage tumors, with a specificity of 90.3 and 96% for the identification of G2-3 and stage Ⅲ-Ⅳ tumors, respectively. On conventional MR sequences, PanNENs have quite a broad spectrum of appearance. Poorly differentiated PanNENs may lack typical MR features, as hypervascularization during the late arterial/pancreatic phase[9]. Kim *et al*[9] and Jang *et al*[11] reported that arterial phase hypointensity was significantly associated with tumors with higher degree of dedifferentiation. We found similar results, as indicated by the higher proportion of G2-3 and stage Ⅲ-Ⅳ tumors among lesions showing hypointensity on late arterial/pancreatic phase images compared to G1 and stage Ⅰ-Ⅱ tumors (69.2% and 75% *vs* 30.8% and 25%, respectively), although without significant differences between groups. In the present study, the presence of heterogeneous enhancement was a good predictor of G2-3 tumors (specificity, 71%); nevertheless, heterogeneous enhancement has been correlated also with tumor size[19] and our results confirms these data: in the present series, PanNENs showing heterogeneous enhancement were significantly larger than homogenous lesions (19.8 mm *vs* 39.3 mm, $P < 0.001$), independently from tumor grade.

DWI appears to be a promising adjunct for the identification of PanNENs and liver metastases, as reported in previous studies[14,20-22]. An inverse correlation between the ADC value and tumor cellularity has been reported in a variety of neoplasms[23-26]: a probable explanation is that increased cellularity causes a decrease in extracellular spaces, which results in restriction of water diffusion. According to the WHO classification, tumor grade in PanNENs is directly linked to tumor cellularity: the higher the degree of cellularity, the poorer the differentiation[1]: theoretically, increased tumor cellularity and reduced cytoplasmic volume will restrict the free motion of water molecules, resulting in a decrease in ADC values[27]. Consistent with this theory, we found that G2-3 PanNENs have significantly lower ADC values compared to G1 tumors (1.09×10^{-3} mm^2/s *vs* 1.45×10^{-3} mm^2/s, $P = 0.003$). Moreover, we found that tumor with higher stage at diagnosis presented significantly lower ADC values (1.10×10^{-3} mm^2/s *vs* 1.53×10^{-3} mm^2/s, $P = 0.001$). ROC analysis determined optimal cut-off values of 1.21 and 1.28×10^{-3} mm^2/s for the identification of G2-3 tumors and stage Ⅲ-Ⅳ tumors, with sensitivity and specificity values of 70.8/80.7% and 64.5/64%, respectively. In the present series, no correlations were found between ADC values and tumor size ($P = 0.236$). Our results therefore may suggest a prognostic role for ADC quantification. Our study has some limitations. First, although we recruited patients who met the inclusion criteria, we cannot rule out a selection bias that may have resulted from the retrospective design of this study. Second, manual measurements of ADC values may be poorly reproducible and unreliable for small lesions due the low spatial resolution of DW images. Finally, extracellular accumulation of collagen, glycosaminoglycans and proteoglycans as well as infiltrating leukocytes may cause restriction of water diffusion in PanNENs in addition to high cellularity: some tumors may present intratumoral fibrosis, and even if well differentiated, they can demonstrate low ADC values. These aspects were explained by Wang *et al*[12], who found a difference in mean ADCs between well-differentiated PanNENs and endocrine carcinomas, but a significant inverse correlation between ADC values and the cellularity of PanNENs was only observed after excluding three well-differentiated tumors with benign behavior and marked fibrosis. It must be otherwise considered that PanNENs containing fibrosis are uncommon; McCall *et al*[28] found only 14% lesions with prominent stromal fibrosis in their large PanNEN series. Further studies, possibly involving intravoxel incoherent motion DW imaging, are needed to better understand the relationship between histopathological features of PanNENs and water diffusivity evaluated with MR-DWI.

In conclusion, our study demonstrated that MR features of PanNENs vary according to the grade of differentiation and the ENETS TNM stage and can predict the biological behavior of these tumors. In particular, irregular margins and low ADC values are good predictors of less-differentiated PanNENs and tumors with higher biological malignancy. MR features may be helpful, in addiction to tissue sampling, to define the most appropriate treatment strategy for PanNENs.

COMMENTS

Background

Pretreatment prediction of the biological behavior of pancreatic neuroendocrine neoplasms (PanNENs) is crucial to determine an efficient treatment strategy for these tumors, especially when unresectable. Nevertheless,

even invasive methods, as fine-needle aspiration (FNA), have a limited accuracy in determining the true proliferative activity of these tumors. Imaging methods could estimate the malignancy of PanNENs in a non-invasive way. Nevertheless, these results are based on small study populations and the diagnostic accuracy of imaging features in predicting the biological behavior of these tumors is still undefined.

Research frontiers

The aims of this study are to describe magnetic resonance (MR) and diffusion-weighted imaging features of PanNENs according to the 2010 World Health Organization grade classification and European Neuroendocrine Tumor Society tumor-nodes-metastases (TNM) staging system by comparing them to histopathology and to determine the accuracy of MR imaging features in predicting the biological behavior of these tumors.

Innovations and breakthroughs

One of the major strenghts of our study is that histopathological analysis was based on surgical specimens, while in most previous study FNA was considered as the external gold standard. This study demonstrated that MR imaging features of PanNENs vary according to the grade of differentiation and the European Neuroendocrine Society TNM stage and can predict the biological behavior of these tumors. In particular, besides other well-known features as liver metastases and vascular infiltration, irregular margins and low apparent diffusion coefficient (ADC) values are good predictors of less-differentiated tumors and of those with higher biological malignancy. MR features may be helpful, in addiction to tissue sampling, to define the most appropriate treatment strategy for PanNENs.

Applications

MR features, especially the mean ADC value calculated by the placement of regions of interest within the tumor, may be helpful, in addiction to tissue sampling, to define the most appropriate treatment strategy for PanNENs.

Peer-review

The paper is well written. The idea of using MR imaging to correlate with the grade/stage of tumors is not novel but in the context of PanNen may provide useful information.

REFERENCES

1 **Rindi G**, Arnold R, Bosman FT. Nomenclature and classification of neuroendocrine neoplasms of the digestive system. In: Bosman FT, Carneiro F, Hruban RH, Theise ND, eds. WHO Classification of Tumors of the Digestive System. 4th ed. Lyon, France: IARC press, 2010; 13

2 **Rindi G**, Falconi M, Klersy C, Albarello L, Boninsegna L, Buchler MW, Capella C, Caplin M, Couvelard A, Doglioni C, Delle Fave G, Fischer L, Fusai G, de Herder WW, Jann H, Komminoth P, de Krijger RR, La Rosa S, Luong TV, Pape U, Perren A, Ruszniewski P, Scarpa A, Schmitt A, Solcia E, Wiedenmann B. TNM staging of neoplasms of the endocrine pancreas: results from a large international cohort study. *J Natl Cancer Inst* 2012; **104**: 764-777 [PMID: 22525418 DOI: 10.1093/jnci/djs208]

3 **Martin-Perez E**, Capdevila J, Castellano D, Jimenez-Fonseca P, Salazar R, Beguiristain-Gomez A, Alonso-Orduña V, Martinez Del Prado P, Villabona-Artero C, Diaz-Perez JA, Monleon A, Marazuela M, Pachon V, Sastre-Valera J, Sevilla I, Castaño A, Garcia-Carbonero R. Prognostic factors and long-term outcome of pancreatic neuroendocrine neoplasms: Ki-67 index shows a greater impact on survival than disease stage. The large experience of the Spanish National Tumor Registry (RGETNE). *Neuroendocrinology* 2013; **98**: 156-168 [PMID: 23988576 DOI: 10.1159/000355152]

4 **Halfdanarson TR**, Rabe KG, Rubin J, Petersen GM. Pancreatic neuroendocrine tumors (PNETs): incidence, prognosis and recent trend toward improved survival. *Ann Oncol* 2008; **19**: 1727-1733 [PMID: 18515795 DOI: 10.1093/annonc/mdn351]

5 **Falconi M**, Eriksson B, Kaltsas G, Bartsch DK, Capdevila J, Caplin M, Kos-Kudla B, Kwekkeboom D, Rindi G, Klöppel G, Reed N, Kianmanesh R, Jensen RT. ENETS Consensus Guidelines Update for the Management of Patients with Functional Pancreatic Neuroendocrine Tumors and Non-Functional Pancreatic Neuroendocrine Tumors. *Neuroendocrinology* 2016; **103**: 153-171 [PMID: 26742109 DOI: 10.1159/000443171]

6 **Rebours V**, Cordova J, Couvelard A, Fabre M, Palazzo L, Vullierme MP, Hentic O, Sauvanet A, Aubert A, Bedossa P, Ruszniewski P. Can pancreatic neuroendocrine tumour biopsy accurately determine pathological characteristics? *Dig Liver Dis* 2015; **47**: 973-977 [PMID: 26169284 DOI: 10.1016/j.dld.2015.06.005]

7 **Takumi K**, Fukukura Y, Higashi M, Ideue J, Umanodan T, Hakamada H, Kanetsuki I, Yoshiura T. Pancreatic neuroendocrine tumors: Correlation between the contrast-enhanced computed tomography features and the pathological tumor grade. *Eur J Radiol* 2015; **84**: 1436-1443 [PMID: 26022520 DOI: 10.1016/j.ejrad.2015.05.005]

8 **Gallotti A**, Johnston RP, Bonaffini PA, Ingkakul T, Deshpande V, Fernández-del Castillo C, Sahani DV. Incidental neuroendocrine tumors of the pancreas: MDCT findings and features of malignancy. *AJR Am J Roentgenol* 2013; **200**: 355-362 [PMID: 23345357 DOI: 10.2214/AJR.11.8037]

9 **Kim JH**, Eun HW, Kim YJ, Lee JM, Han JK, Choi BI. Pancreatic neuroendocrine tumour (PNET): Staging accuracy of MDCT and its diagnostic performance for the differentiation of PNET with uncommon CT findings from pancreatic adenocarcinoma. *Eur Radiol* 2016; **26**: 1338-1347 [PMID: 26253257 DOI: 10.1007/s00330-015-3941-7]

10 **Rodallec M**, Vilgrain V, Couvelard A, Rufat P, O'Toole D, Barrau V, Sauvanet A, Ruszniewski P, Menu Y. Endocrine pancreatic tumours and helical CT: contrast enhancement is correlated with microvascular density, histoprognostic factors and survival. *Pancreatology* 2006; **6**: 77-85 [PMID: 16327283 DOI: 10.1159/000090026]

11 **Jang KM**, Kim SH, Lee SJ, Choi D. The value of gadoxetic acid-enhanced and diffusion-weighted MRI for prediction of grading of pancreatic neuroendocrine tumors. *Acta Radiol* 2014; **55**: 140-148 [PMID: 23897307 DOI: 10.1177/0284185113494982]

12 **Wang Y**, Chen ZE, Yaghmai V, Nikolaidis P, McCarthy RJ, Merrick L, Miller FH. Diffusion-weighted MR imaging in pancreatic endocrine tumors correlated with histopathologic characteristics. *J Magn Reson Imaging* 2011; **33**: 1071-1079 [PMID: 21509863 DOI: 10.1002/jmri.22541]

13 **Hwang EJ**, Lee JM, Yoon JH, Kim JH, Han JK, Choi BI, Lee KB, Jang JY, Kim SW, Nickel MD, Kiefer B. Intravoxel incoherent motion diffusion-weighted imaging of pancreatic neuroendocrine tumors: prediction of the histologic grade using pure diffusion coefficient and tumor size. *Invest Radiol* 2014; **49**: 396-402 [PMID: 24500090 DOI: 10.1097/RLI.0000000000000028]

14 **De Robertis R**, D'Onofrio M, Zamboni G, Tinazzi Martini P, Gobbo S, Capelli P, Butturini G, Girelli R, Ortolani S, Cingarlini S, Pederzoli P, Scarpa A. Pancreatic Neuroendocrine Neoplasms: Clinical Value of Diffusion-Weighted Imaging. *Neuroendocrinology* 2016; **103**: 758-770 [PMID: 26646652 DOI: 10.1159/000442984]

15 **Rindi G**, Klöppel G, Alhman H, Caplin M, Couvelard A, de Herder WW, Erikssson B, Falchetti A, Falconi M, Komminoth P, Körner M, Lopes JM, McNicol AM, Nilsson O, Perren A, Scarpa A, Scoazec JY, Wiedenmann B. TNM staging of foregut (neuro)endocrine tumors: a consensus proposal including a grading system. *Virchows Arch* 2006; **449**: 395-401 [PMID: 16967267 DOI: 10.1007/s00428-006-0250-1]

16 **Pezzilli R**, Partelli S, Cannizzaro R, Pagano N, Crippa S, Pagnanelli M, Falconi M. Ki-67 prognostic and therapeutic decision driven marker for pancreatic neuroendocrine neoplasms (PNENs): A systematic review. *Adv Med Sci* 2016; **61**: 147-153 [PMID: 26774266 DOI: 10.1016/j.advms.2015.10.001]

17 **Strosberg J**, Nasir A, Coppola D, Wick M, Kvols L. Correlation between grade and prognosis in metastatic gastroenteropancreatic neuroendocrine tumors. *Hum Pathol* 2009; **40**: 1262-1268 [PMID: 19368957 DOI: 10.1016/j.humpath.2009.01.010]

18 **Yang M**, Zeng L, Zhang Y, Wang WG, Wang L, Ke NW, Liu XB,

Tian BL. TNM staging of pancreatic neuroendocrine tumors: an observational analysis and comparison by both AJCC and ENETS systems from 1 single institution. *Medicine* (Baltimore) 2015; **94**: e660 [PMID: 25816036 DOI: 10.1097/MD.0000000000000660]

19 **Hyodo R**, Suzuki K, Ogawa H, Komada T, Naganawa S. Pancreatic neuroendocrine tumors containing areas of iso- or hypoattenuation in dynamic contrast-enhanced computed tomography: Spectrum of imaging findings and pathological grading. *Eur J Radiol* 2015; **84**: 2103-2109 [PMID: 26321494 DOI: 10.1016/j.ejrad.2015.08.014]

20 **Schmid-Tannwald C**, Schmid-Tannwald CM, Morelli JN, Neumann R, Haug AR, Jansen N, Nikolaou K, Schramm N, Reiser MF, Rist C. Comparison of abdominal MRI with diffusion-weighted imaging to 68Ga-DOTATATE PET/CT in detection of neuroendocrine tumors of the pancreas. *Eur J Nucl Med Mol Imaging* 2013; **40**: 897-907 [PMID: 23460395 DOI: 10.1007/s00259-013-2371-5]

21 **Farchione A**, Rufini V, Brizi MG, Iacovazzo D, Larghi A, Massara RM, Petrone G, Poscia A, Treglia G, De Marinis L, Giordano A, Rindi G, Bonomo L. Evaluation of the Added Value of Diffusion-Weighted Imaging to Conventional Magnetic Resonance Imaging in Pancreatic Neuroendocrine Tumors and Comparison With 68Ga-DOTANOC Positron Emission Tomography/Computed Tomography. *Pancreas* 2016; **45**: 345-354 [PMID: 26418904 DOI: 10.1097/MPA.0000000000000461]

22 **d'Assignies G**, Fina P, Bruno O, Vullierme MP, Tubach F, Paradis V, Sauvanet A, Ruszniewski P, Vilgrain V. High sensitivity of diffusion-weighted MR imaging for the detection of liver metastases from neuroendocrine tumors: comparison with T2-weighted and dynamic gadolinium-enhanced MR imaging. *Radiology* 2013; **268**: 390-399 [PMID: 23533288 DOI: 10.1148/radiol.13121628]

23 **Higano S**, Yun X, Kumabe T, Watanabe M, Mugikura S, Umetsu A, Sato A, Yamada T, Takahashi S. Malignant astrocytic tumors: clinical importance of apparent diffusion coefficient in prediction of grade and prognosis. *Radiology* 2006; **241**: 839-846 [PMID: 17032910 DOI: 10.1148/radiol.2413051276]

24 **Humphries PD**, Sebire NJ, Siegel MJ, Olsen ØE. Tumors in pediatric patients at diffusion-weighted MR imaging: apparent diffusion coefficient and tumor cellularity. *Radiology* 2007; **245**: 848-854 [PMID: 17951348 DOI: 10.1148/radiol.2452061535]

25 **Muhi A**, Ichikawa T, Motosugi U, Sano K, Matsuda M, Kitamura T, Nakazawa T, Araki T. High-b-value diffusion-weighted MR imaging of hepatocellular lesions: estimation of grade of malignancy of hepatocellular carcinoma. *J Magn Reson Imaging* 2009; **30**: 1005-1011 [PMID: 19856432 DOI: 10.1002/jmri.21931]

26 **Hayashida Y**, Yakushiji T, Awai K, Katahira K, Nakayama Y, Shimomura O, Kitajima M, Hirai T, Yamashita Y, Mizuta H. Monitoring therapeutic responses of primary bone tumors by diffusion-weighted image: Initial results. *Eur Radiol* 2006; **16**: 2637-2643 [PMID: 16909220 DOI: 10.1007/s00330-006-0342-y]

27 **Takahashi Y**, Akishima-Fukasawa Y, Kobayashi N, Sano T, Kosuge T, Nimura Y, Kanai Y, Hiraoka N. Prognostic value of tumor architecture, tumor-associated vascular characteristics, and expression of angiogenic molecules in pancreatic endocrine tumors. *Clin Cancer Res* 2007; **13**: 187-196 [PMID: 17200354 DOI: 10.1158/1078-0432.CCR-06-1408]

28 **McCall CM**, Shi C, Klein AP, Konukiewitz B, Edil BH, Ellison TA, Wolfgang CL, Schulick RD, Klöppel G, Hruban RH. Serotonin expression in pancreatic neuroendocrine tumors correlates with a trabecular histologic pattern and large duct involvement. *Hum Pathol* 2012; **43**: 1169-1176 [PMID: 22221702 DOI: 10.1016/j.humpath.2011.09.014]

P- Reviewer: Peng SY, Stephen RM **S- Editor**: Qi Y **L- Editor**: A
E- Editor: Zhang FF

Published by **Baishideng Publishing Group Inc**
8226 Regency Drive, Pleasanton, CA 94588, USA
Telephone: +1-925-223-8242
Fax: +1-925-223-8243
E-mail: bpgoffice@wjgnet.com
Help Desk: http://www.wjgnet.com/esps/helpdesk.aspx
http://www.wjgnet.com

ISSN 1007-9327
0 2>